ISSN 1948-9366 (online)

World Journal of *Gastrointestinal Surgery*

World J Gastrointest Surg 2024 July 27; 16(7): 1956-2364

Published by Baishideng Publishing Group Inc

World Journal of Gastrointestinal Surgery

Contents

Monthly Volume 16 Number 7 July 27, 2024

EDITORIAL

REVIEW

ORIGINAL ARTICLE

Case Control Study

Retrospective Cohort Study

World Journal of Gastrointestinal Surgery

Monthly Volume 16 Number 7 July 27, 2024

Contents

Retrospective Study

World Journal of Gastrointestinal Surgery

Monthly Volume 16 Number 7 July 27, 2024

Contents

World Journal of Gastrointestinal Surgery

Monthly Volume 16 Number 7 July 27, 2024

Contents

ABOUT COVER

Peer Reviewer of *World Journal of Gastrointestinal Surgery*, Hideki Aoki, MD, PhD, Chief Doctor, Surgeon, Department of Surgery, Iwakuni Clinical Center, Iwakuni 740-8510, Japan. aoki.hideki.hy@mail.hosp.go.jp

AIMS AND SCOPE

The primary aim of *World Journal of Gastrointestinal Surgery* (*WJGS*, *World J Gastrointest Surg*) is to provide scholars and readers from various fields of gastrointestinal surgery with a platform to publish high-quality basic and clinical research articles and communicate their research findings online.

WJGS mainly publishes articles reporting research results and findings obtained in the field of gastrointestinal surgery and covering a wide range of topics including biliary tract surgical procedures, biliopancreatic diversion, colectomy, esophagectomy, esophagostomy, pancreas transplantation, and pancreatectomy, *etc.*

INDEXING/ABSTRACTING

The *WJGS* is now abstracted and indexed in Science Citation Index Expanded (SCIE, also known as SciSearch®), Current Contents/Clinical Medicine, Journal Citation Reports/Science Edition, PubMed, PubMed Central, Reference Citation Analysis, China Science and Technology Journal Database, and Superstar Journals Database. The 2024 Edition of Journal Citation Reports® cites the 2023 journal impact factor (JIF) for *WJGS* as 1.8; JIF without journal self cites: 1.7; 5-year JIF: 1.9; JIF Rank: 123/290 in surgery; JIF Quartile: Q2; and 5-year JIF Quartile: Q3.

RESPONSIBLE EDITORS FOR THIS ISSUE

NAME OF JOURNAL
World Journal of Gastrointestinal Surgery

ISSN
ISSN 1948-9366 (online)

LAUNCH DATE
November 30, 2009

FREQUENCY
Monthly

EDITORS-IN-CHIEF
Peter Schemmer

EDITORIAL BOARD MEMBERS
https://www.wjgnet.com/1948-9366/editorialboard.htm

PUBLICATION DATE
July 27, 2024

INSTRUCTIONS TO AUTHORS
https://www.wjgnet.com/bpg/gerinfo/204

GUIDELINES FOR ETHICS DOCUMENTS
https://www.wjgnet.com/bpg/GerInfo/287

GUIDELINES FOR NON-NATIVE SPEAKERS OF ENGLISH
https://www.wjgnet.com/bpg/gerinfo/240

PUBLICATION ETHICS
https://www.wjgnet.com/bpg/GerInfo/288

PUBLICATION MISCONDUCT
https://www.wjgnet.com/bpg/gerinfo/208

ARTICLE PROCESSING CHARGE
https://www.wjgnet.com/bpg/gerinfo/242

STEPS FOR SUBMITTING MANUSCRIPTS
https://www.wjgnet.com/bpg/GerInfo/239

ONLINE SUBMISSION
https://www.f6publishing.com

World Journal of Gastrointestinal Surgery

Submit a Manuscript: https://www.f6publishing.com

World J Gastrointest Surg 2024 July 27; 16(7): 2281-2295

DOI: 10.4240/wjgs.v16.i7.2281

ISSN 1948-9366 (online)

ORIGINAL ARTICLE

Clinical and Translational Research

Construction of prognostic markers for gastric cancer and comprehensive analysis of pyroptosis-related long non-coding RNAs

Yu Wang, Di Li, Jing Xun, Yu Wu, Hong-Lei Wang

Specialty type: Gastroenterology and hepatology

Provenance and peer review: Unsolicited article; Externally peer reviewed.

Peer-review model: Single blind

Peer-review report's classification

Scientific Quality: Grade B
Novelty: Grade B
Creativity or Innovation: Grade B
Scientific Significance: Grade B

P-Reviewer: Iida T

Received: April 10, 2024
Revised: May 22, 2024
Accepted: June 14, 2024
Published online: July 27, 2024
Processing time: 102 Days and 23.9 Hours

Yu Wang, Di Li, Jing Xun, Yu Wu, Hong-Lei Wang, Department of Gastrointestinal Surgery, Hospital of Integrated Chinese and Western Medicine, Tianjin University, Tianjin 300100, China

Corresponding author: Hong-Lei Wang, Doctor, Chief Physician, Department of Gastrointestinal Surgery, Hospital of Integrated Chinese and Western Medicine, Tianjin University, No. 6 Changjiang Road, Nankai District, Tianjin 300100, China.
hongleiwang0319@outlook.com

Abstract

BACKGROUND

China's most frequent malignancy is gastric cancer (GC), which has a very poor survival rate, and the survival rate for patients with advanced GC is dismal. Pyroptosis has been connected to the genesis and development of cancer. The function of pyroptosis-related long non-coding RNAs (PRLs) in GC, on the other hand, remains uncertain.

AIM

To explore the construction and comprehensive analysis of the prognostic characteristics of long non-coding RNA (lncRNA) related to pyroptosis in GC patients.

METHODS

The TCGA database provided us with 352 stomach adenocarcinoma samples, and we obtained 28 pyroptotic genes from the Reactome database. We examined the correlation between lncRNAs and pyroptosis using the Pearson correlation coefficient. Prognosis-related PRLs were identified through univariate Cox analysis. A predictive signature was constructed using stepwise Cox regression analysis, and its reliability and independence were assessed. To facilitate clinical application, a nomogram was created based on this signature. we analyzed differences in immune cell infiltration, immune function, and checkpoints between the high-risk group (HRG) and low-risk group (LRG).

RESULTS

Five hundred and twenty-three PRLs were screened from all lncRNAs (absolute correlation coefficient > 0.4, $P < 0.05$). Nine PRLs were included in the risk prediction signature that was created through stepwise Cox regression analysis. We determined the risk score for GC patients and employed the median value as the dividing line between HRG and LRG. The ability of the risk signature to

predict the overall survival (OS) of GC is demonstrated by the Kaplan-Meier analysis, risk curve, receiver operating characteristic curve, and decision curve analysis curve. The risk signature was shown to be an independent prognostic factor for OS in both univariate and multivariate Cox regression analyses. HRG showed a more efficient local immune response or modulation compared to LRG, as indicated by the predicted signal pathway analysis and examination of immune cell infiltration, function, and checkpoints ($P < 0.05$).

CONCLUSION

In general, we have created a brand-new prognostic signature using PRLs, which may provide ideas for immunotherapy in patients with GC.

Key Words: Gastric cancer; Pyroptosis; Prognosis; Immune checkpoint; Long non-coding RNA; Immune cell infiltrating

Core Tip: In this study, China's most common malignancy is gastric cancer (GC), which has a poor survival rate. Pyroptosis is connected to cancer development. The function of pyroptosis-related long non-coding RNAs (PRLs) in GC is uncertain. In our study, we took advantage of the 352 gastric adenocarcinoma samples included in the TCGA database and obtained data on 28 cases related to the pyroptotic genes from the Reactome database. We used the Pearson correlation coefficient method to screen out the long non-coding RNAs associated with pyroptosis. Using univariate Cox analysis, we identified the PRL associated with prognosis. By using PRLs, we created a completely new prognostic marker, which may provide ideas for immunotherapy in GC patients.

Citation: Wang Y, Li D, Xun J, Wu Y, Wang HL. Construction of prognostic markers for gastric cancer and comprehensive analysis of pyroptosis-related long non-coding RNAs. *World J Gastrointest Surg* 2024; 16(7): 2281-2295
URL: https://www.wjgnet.com/1948-9366/full/v16/i7/2281.htm
DOI: https://dx.doi.org/10.4240/wjgs.v16.i7.2281

INTRODUCTION

In 2020, there were more than 1000000 new instances of gastric cancer (GC) and approximately 770000 deaths from GC, based on the Global Cancer Statistics[1]. But GC is hard to detect early, as usually asymptomatic in the early stage. As a result, about 70% of GC patients receive an advanced diagnosis[2]. Approximately 95% of GC are adenocarcinomas[3]. In recent years, Despite the rapid development of radiotherapy, chemotherapy, and immunotherapy, surgical resection of the malignant lesion is the mainstay therapy for GC[4,5]. With such a multidisciplinary treatment approach, the survival rate for advanced GC is still less than 10%[6]. Consequently, there is still a pressing need to investigate new biomarkers for GC patient prognosis prediction.

Cell death mainly includes programmed and non-programmed death, and pyroptosis is pro-inflammatory programmed cell death. The Greek words "pyro" and "ptosis," which denote fever and recession, respectively, are found in the word "pyroptosis"[7]. The ballooning of the cell and multiple processes on the surface of the cell membrane before rupture set pyroptosis apart from apoptosis. The canonical inflammasome pathway and the noncanonical inflammasome pathway are the two primary pathway branches that usually makeup pyroptosis signaling[8]. When cells are menaced by a variety of pathogens, such as bacteria, viruses, fungi, and protozoa, cytosolic pattern recognition receptors identify pathogen-associated molecular patterns and danger-associated molecular patterns. Consequently, it causes proteins farther down the chain to organize into inflammatory bodies and activate caspase-1 or caspase-11/4/5. Gasdermin D (GSDMD) is cleaved by caspase, and the N-terminal domain of GSDMD oligomerizes to generate membrane holes, releasing IL-1 and IL-18 and causing cell pyroptotic death[9,10]. In the noncanonical inflammasome pathway, lipopolysaccharide actives caspase-4/-5/-11 to induce cell pyroptotic death[11].

Pyroptosis is crucial for the onset and progression of many illnesses, including cancers, metabolic disorders, infectious diseases, nerve-related diseases, and atherosclerosis[12]. According to earlier research, pyroptosis, and cancer formation and progression are tightly related. For instance, Rogers *et al*[12] discovered that in melanoma, knocking down Gasdermin E in the B16-Ova cell line greatly decreases the release of cytochrome c and the activation of caspase-3 and speeds up tumor development[12]. By triggering the pyroptosis pathway at the gene and protein levels, 4-hydroxybenzoic acid was able to stop the growth of a non-small cell lung cancer cell line, according to research by Sannino *et al*[13]. In colon cancer, silencing Gasdermin C was revealed to suppress colon cancer cell line proliferation and metastasis, while overexpression of Gasdermin C can enhance cell proliferation[14,15]. The high expression of cytokine IL-1β leads to the recruitment of Myeloid-derived suppressor cells in the stomach, which increases the risk of spontaneous gastritis and GC[16]. In addition, a lot of studies on leukemia, uterine cancer, and liver cancer have shown that pyroptosis is closely related to the incidence and progression of carcinoma[17-21].

A transcript with a length of more than 200 nucleotides known as a long non-coding RNA (lncRNA) cannot produce a protein yet has a distinct expression in numerous tissues, including malignancies[22,23]. More than 28000 LncRNA are thought to be encoded in the human genome, and there is still much to be uncovered[24]. LncRNA not only participates in chromatin interaction, transcriptional regulation, and RNA processing but also regulates the stability or translation process of mRNA and affects cell signal cascades[25]. In recent years, more and more research has revealed that lncRNA can regulate the biological functions of tumor proliferation, apoptosis, invasion, and metastasis in multiple signal pathways[26,27]. For instance, PCGEM1 is a lncRNA that is strongly androgen-regulated and tissue-specific to the prostate[28]. In prostate cancer, overexpression of PCGEM1 may increase cellular resistance to chemotherapy by promoting cell growth and clone creation[29,30]. The capacity of human breast cancer cells to metastasize to the lungs is improved by lncRNA MALAT1 knockout while restoring MALAT1 expression weakens the metastatic capability[31]. GC has a greater degree of HOTAIR expression than the nearby normal tissues. Patients with diffuse GC who express more HOTAIR would have increased venous invasion, local lymph node metastases, and a decreased chance of survival. Overexpression of HOTAIR could promote liver metastasis in GC[32]. In addition to the above, publications on the function and mechanism of lncRNA in different malignancies are growing. The pattern of lncRNA expression and its role in GC, however, have not been thoroughly examined.

Although some researchers have shown that lncRNA has a special function in the pyroptosis of GC, little research has been done on this topic, and the precise mechanism is not yet fully understood[33]. Using the pyroptosis-related lncRNA (PRL) collected from The Cancer Genome Atlas (TCGA) database, we developed a signature to predict the prognosis of GC patients. The findings might serve as a guide for doctors treating GC patients and evaluating their prognosis.

MATERIALS AND METHODS

Acquisition and processing of data

We concurrently downloaded the clinical data corresponding to the gastric adenocarcinoma expression data from the TCGA database (GDC, cancer.gov). This research comprised 352 patients in total for a follow-up study.

Identification of prognosis-related PRLs

According to the gene annotation in the expression data of 352 GC cases, 13824 LncRNA were obtained. Twenty-eight genes associated with pyroptosis were collected from the Reactome Pathway Database (Home - Reactome Pathway Database). The Pearson correlation coefficient assessed correlations between pyroptosis-related genes and lncRNA. PRLs were characterized as lncRNAs with an absolute correlation coefficient > 0.4 and $P < 0.05$, and a total of 532 PRLs were chosen. To identify PRLs that were associated with prognosis, we used univariate Cox regression analysis. Twenty-eight LncRNA with prognostic values related to pyroptosis were further screened ($P < 0.05$).

Prognostic signature and nomogram construction based on PRLs

For the above 28 PRLs, based on stepwise Cox regression analysis, a further prediction signature was established, including nine PRLs. Risk scores were calculated for each patient based on the normalized expression levels of lncRNAs and their related regression coefficients. This is the method used to determine the risk score: Risk score = sum (lncRNA expression level corresponding coefficient). We created and displayed the co-expression network between nine PRLs and associated pyroptotic genes using the Cytoscape program. In parallel, we developed a Nomogram for clinical use to forecast GC patients' 1, 3, and 5-year survival rates.

Examining prognostic signature clinical benefits

We determined a risk score for each GC patient using the prognostic signature described above and using the median risk score as a cutoff, we separated patients into a low-risk Group (LRG) and a high-risk group (HRG). We used decision curve analysis (DCA) and evaluated the prognostic signature's areas under the receiver operating characteristic (ROC) curve at 1, 2, and 3 years to assess the precision and dependability of the risk signature. To demonstrate the risk score's ability to predict outcomes, the Kaplan-Meier (K-M) survival curves were shown using the R software. Simultaneously, we plotted risk curves and heat maps of lncRNA expression for HRG and LRG. To determine if risk score was an independent prognostic predictor, univariate and multivariate Cox regression analyses were carried out, and a forest plot was shown.

Analysis of differential expression and functional enrichment

We examined the biological functions of differential genes between HRG and LRG. Possible underlying mechanisms were explored by KEGG and GO enrichment analysis. We also looked at the association between risk scores and clinical variables.

Immune infiltration and immune function analysis

We utilized six methods (TIMER[34], CIBERSORT[35], quanTIseq[36], MCP-counter[37], xCell[38], and EPIC[39]) to figure out the number of infiltrating immune cells across HRG and LRG. Finally, we examined immune checkpoint-related gene expression levels and immune function variations in HRG and LRG, offering therapeutic therapy alternatives.

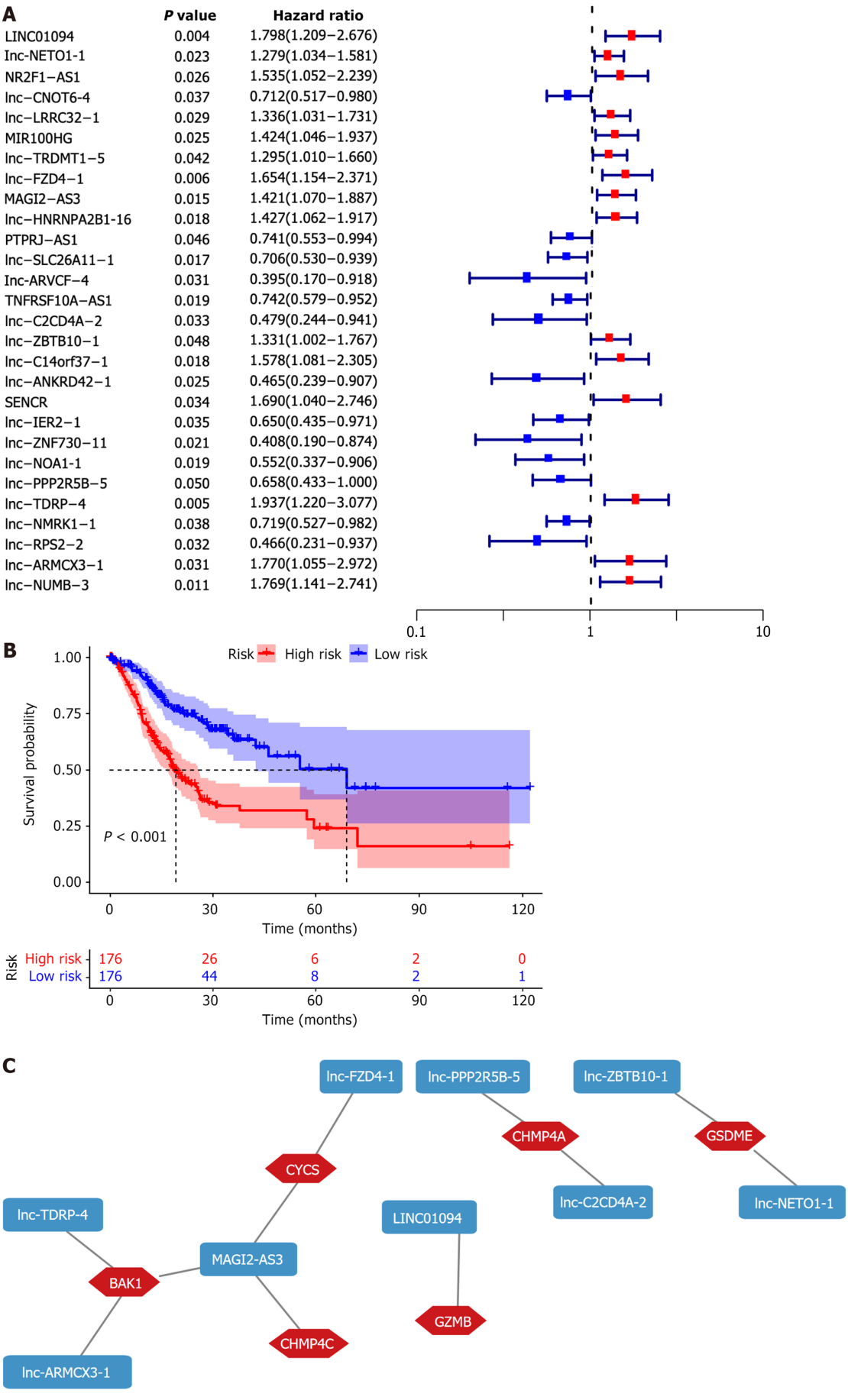

Figure 1 Establishing a risk signature. A: Univariate cox regression analysis was used to identify 28 pyroptosis-related long non-coding RNAs (PRLs)

associated with prognosis; B: Patients were divided into high-risk group (HRG) and low-risk group, and a Kaplan-Meier analysis showed that the HRG's prognosis was worse ($P < 0.001$); C: Cytoscape visualized the coexpression network between nine PRLs and pyroptosis genes.

RESULTS

lncRNA identification of PRLs in GC

This research comprised 352 GC patients in total. We performed Pearson correlation analysis on 28 pyroptosis genes obtained from the database and lncRNAs in GC patients and received 532 PRLs (absolute correlation coefficient > 0.4, $P < 0.05$). Twenty-eight lncRNAs were substantially related to survival, according to further univariate regression analysis ($P < 0.05$; Figure 1A).

Construction of GC prognosis PRLs signature

Using stepwise Cox regression analysis, we further filtered nine PRLs from the 28 lncRNAs based on the aforementioned 28 PRLs. These lncRNAs are the most effective risk marker for GC patients' prognosis (Table 1). This is the procedure for calculating the risk score: Risk score = sum (lncRNA expression level a corresponding coefficient). We determined each GC patient's risk score using the algorithm above and used a median value to split the population into HRG and LRG. According to the K-M survival analysis, HRG patients had significantly lower survival times than LRG patients, demonstrating that these nine lncRNAs had prognostic significance (Figure 1B). The co-expression network between the nine PRLs and the related pyroptosis genes was viewed using the Cytoscape program (Figure 1C).

Table 1 Signature-included pyroptosis-related long non-coding RNAs

LncRNA	Coefficient	HR	HR, 95%CI (lower)	HR, 95%CI (upper)
LINCO1094	0.779872703	2.181194588	1.36366574	3.48883871
Inc-NETO1-1	0.23660583	1.266941629	1.005091889	1.597009298
Inc-FZD4-1	0.680754207	1.975367005	1.12519373	3.467913749
MAGI2-AS3	-0.674642651	0.5093384	0.272837933	0.95084141
Inc-C2CD4A-2	-1.001548394	0.36731026	0.164990512	0.81772476
Inc-ZBTB10-1	0.441911848	1.555678598	1.078798355	2.243362615
Inc-PPP2R5B-5	-0.40825843	0.66480705	0.389416283	1.134951037
Inc-TDRP-4	0.900439987	2.460685544	1.248752759	4.848816788
Inc-ARMCX3-1	0.616084855	1.851664298	0.955899247	3.586843157

LncRNA: Long non-coding RNA; HR: Hazard ratio.

Evaluate the reliability and accuracy of risk signature

We drew the risk curves and expression profiles of nine PRLs using the R software program. From the distribution of risk scores and the patients' survival status, the longer the survival time, the lower the risk score (Figure 2A and B). The expression levels of LINC01094, lnc-NETO1-1, lnc-FZD4-1, MAGI2-AS3, lnc-ZBTB10-1, and-TDRP-4, and lnc-ARMCX3-1 were greater in the HRG than the LRG among these nine lncRNA expression profiles, whereas lnc-C2CD4A-2 and lnc-PPP2R5B-5 were the opposite (Figure 2C). The risk signature was considerably superior to clinical features for predicting the prognosis of GC patients, according to ROC curve analyses (Figure 2D). The survival prognosis areas under the ROC curves (AUCs) at 1, 2, and 3 years were, respectively, 0.678, 0.692, and 0.702 (Figure 2E). The risk signature was considerably superior to clinical features for predicting the prognosis of GC patients, DCA curve analyses (Figure 2F).

Value of risk scores as an independent predictor

We conducted univariate and multivariate Cox analyses on risk score and several clinical characteristics [age, sex, clinical stage, distant metastasis (M stage), lymph node metastasis (N stage), and tumor size (T stage)] to ascertain if risk score may be a standalone prognostic factor impacting GC patients' survival. The results demonstrate that the risk score was a statistically meaningful prognostic factor and might be utilized independently [$P < 0.001$, HR 1.923, 95%CI: (1.614-2.292), $P < 0.001$, HR 1.954, 95%CI: (1.617-2.362); Figure 3A and B]. Clinicians may not be able to effectively use the risk score calculation due to its complexity. As a result, we create a visual nomogram for ease of use based on the risk calculation mentioned above and clinical variables (age and clinical stage; Figure 3C).

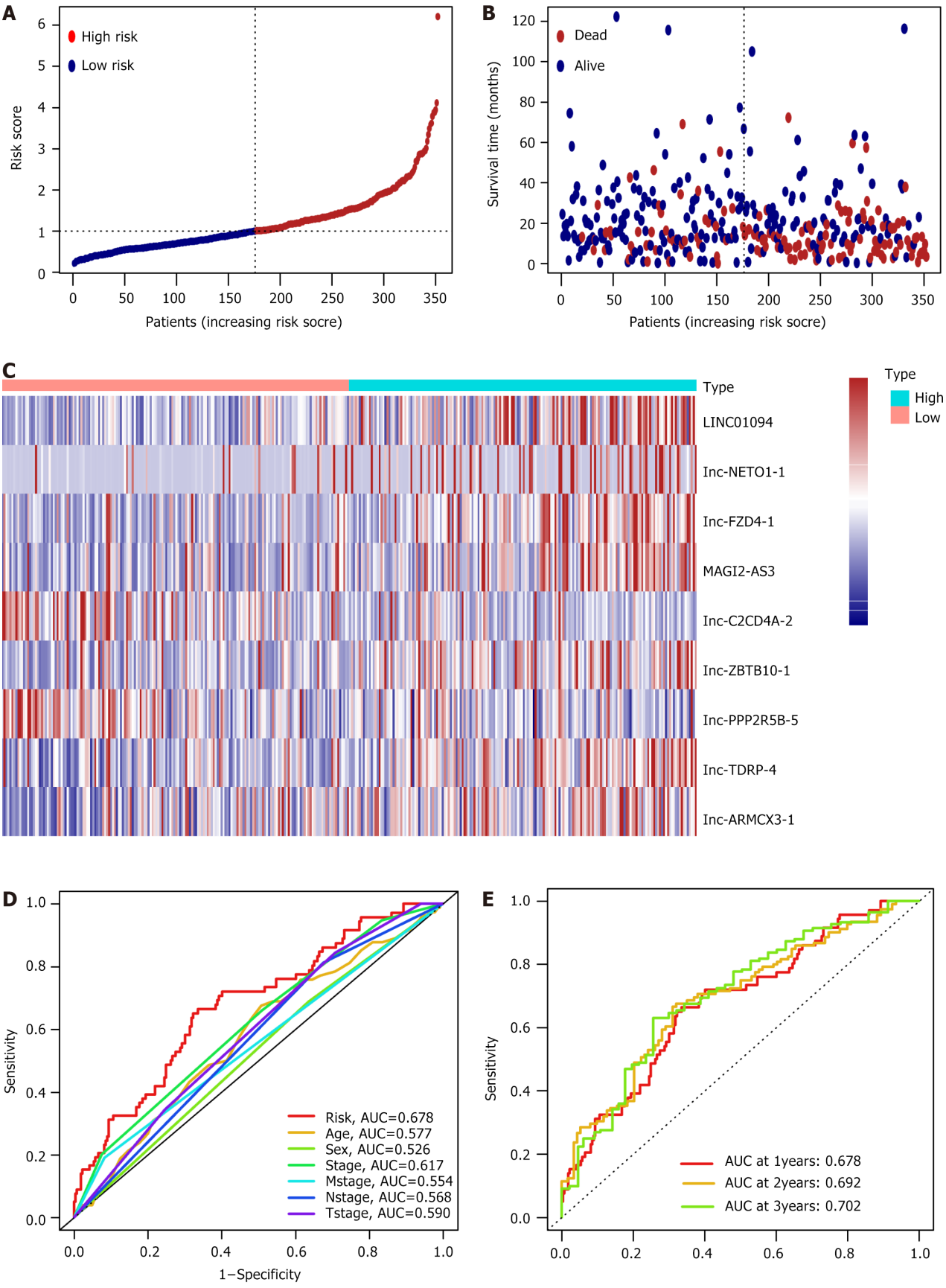
A
High risk
Low risk
Risk score
Patients (increasing risk socre)
B
Dead
Alive
Survival time (months)
Patients (increasing risk socre)
C
Type
LINC01094
Inc-NETO1-1
Inc-FZD4-1
MAGI2-AS3
Inc-C2CD4A-2
Inc-ZBTB10-1
Inc-PPP2R5B-5
Inc-TDRP-4
Inc-ARMCX3-1
Type
High
Low
D
Sensitivity
1−Specificity
Risk, AUC=0.678
Age, AUC=0.577
Sex, AUC=0.526
Stage, AUC=0.617
Mstage, AUC=0.554
Nstage, AUC=0.568
Tstage, AUC=0.590
E
Sensitivity
AUC at 1years: 0.678
AUC at 2years: 0.692
AUC at 3years: 0.702

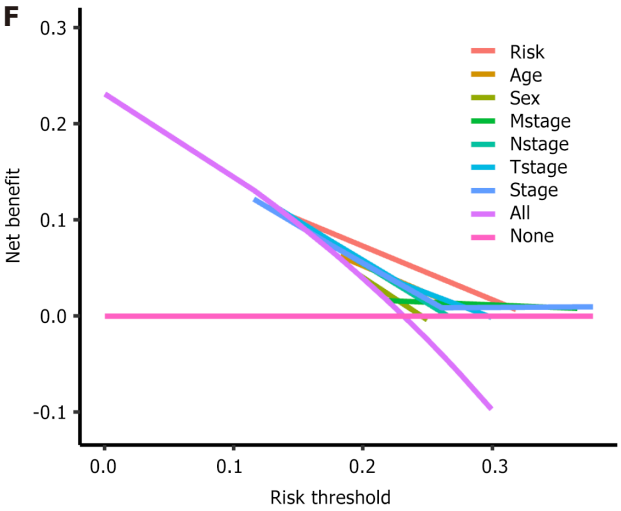

Figure 2 Evaluate reliability and accuracy of risk signature. A and B: The dispersion of patients' survival conditions and risk scores revealed that as the risk score rose, more people died; C: Nine pyroptosis-related long non-coding RNAs' expression heatmap between high-risk group and low-risk group; D: Age, sex, clinical stage, distant metastasis, lymph node metastasis, and tumor size had lower reliability than the risk signature; E: By doing a 1-, 2-, and 3-year receiver operating characteristic analysis, the prognostic utility of the risk signature was confirmed; F: Decision curve analysis was used to assess the dependability of the risk signature.

Analysis of differentially expressed genes in high- and low-risk groups for functional enrichment

To investigate the possible biological roles of genes that are expressed differently in HRG and LRG of GC patients. We searched for mRNAs that differed in expression across HRG and LRG using an R software program. Differential expression mRNAs were mostly enriched in the PI3K-Akt signaling pathway and invasion and metastasis-related pathways, including focal adhesion, ECM-receptor interaction, and regulation of the actin cytoskeleton, in the KEGG enrichment analysis (Figure 4A). The above mRNAs were discovered to be enriched in extracellular matrix-related pathways, such as extracellular matrix structural constituent, collagen binding, extracellular matrix organization, and extracellular structure organization. They were also linked to immune responses, such as antigen binding, immunoglobulin complex, and humoral immune response mediated by circulating immunoglobulin, according to GO enrichment analysis (Figure 4B). These findings point in the right direction for deducing the underlying mechanism between PRL and GC and show substantial molecular functional variations between HRG and LRG of GC. We also investigated any variations in the clinical characteristics of patients across HRG and LRG. For this purpose, we compared sex, TNM stage, and age. T and N showed substantial differences ($P < 0.05$). The higher the risk, the higher the T and N stages of GC, and the worse the prognosis (Figure 4C).

Detailed examination of immune cell infiltration in HRG and LRG

We employed six methods to compute and map the immune cell infiltration Heatmap to assess if there are variations in immune cell infiltration across HRG and LRG. (Figure 5A). The majority of immune function scores were statistically significantly higher in the HRG, as shown by an analysis of immune function differences (Figure 5B). Only LGALS9 and TNFRSF14 had greater expressions in the LRG, according to our additional analysis of the expression levels of immune checkpoints between HRG and LRG. In the HRG, several immune checkpoints, like PDCD1LG2 (PD-L2), TIGIT, BTLA, CD40, and CD80, were strongly expressed (Figure 5C).

DISCUSSION

Globally, GC is one of the tumors with the highest rates of morbidity and death. However, the vast majority of patients are identified at an advanced stage, and the median overall survival (OS) for advanced GC is only approximately eight months[40,41]. Therefore, it is critical to investigate new accurate biomarkers for GC diagnosis, therapy, and prognosis. Pyroptosis is a kind of programmed cell death that is crucial to the onset and progression of many illnesses, including cancer. There are few studies on PRLs in GC, so it will be of great value to construct a prognostic signature composed of PRLs.

We initially identified 28 PRLs from the TCGA database of gastric adenocarcinoma patients using univariate Cox analysis to select hallmark PRLs linked to GC prognosis (Figure 1A). The nine most useful PRLs were then collected by a stepwise Cox regression analysis, and a risk signature was created. These nine PRLs were LINC01094, lnc-NETO1-1, lnc-FZD4-1, MAGI2-AS3, lnc- ZBTB10-1, lnc-TDRP-4, lnc-ARMCX3-1, lnc-C2CD4A-2 and lnc-PPP2R5B-5 (Table 1). To evaluate the accuracy of the signature, patients were separated into HRG and LRG based on the median risk score (Figure 2A). The findings indicated that the prognosis was worse for the HRG than for the LRG (Figures 1B and 2B). The risk score AUC was 0.678 when combined with six regularly used clinical features, which was considerably higher than

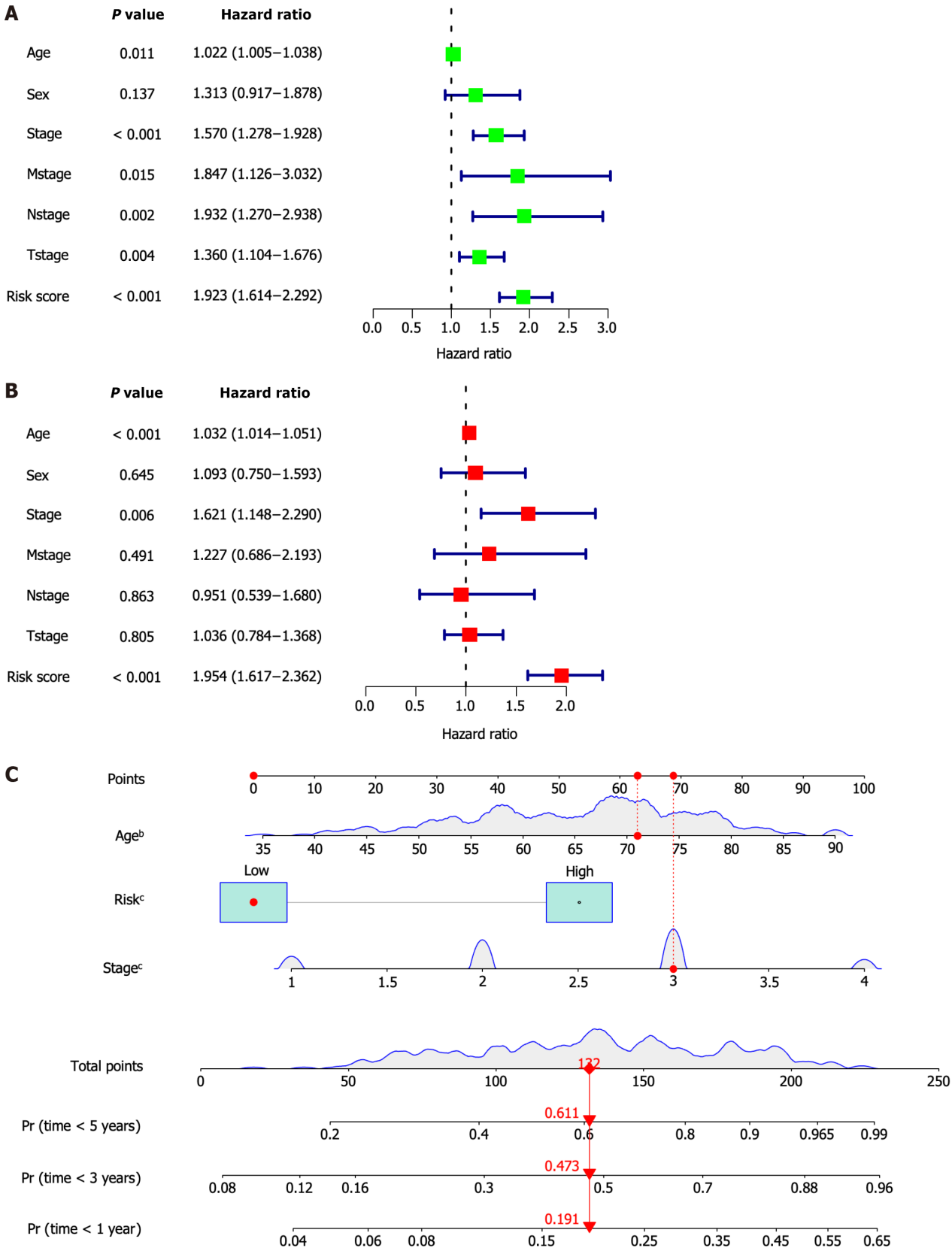

Figure 3 The risk signature's independent prognostic value and nomogram development. A: Age, clinical stage, distant metastasis (M), lymph node metastasis (N), tumor size (T), and risk score all exhibited prognostic significance, according to a univariate Cox regression analysis; B: Age and risk score may be independent predictors of outcome, according to multivariate Cox regression analysis; C: The clinical stage and the risk score were combined to create a nomogram. [b]$P < 0.01$, [c]$P < 0.001$.

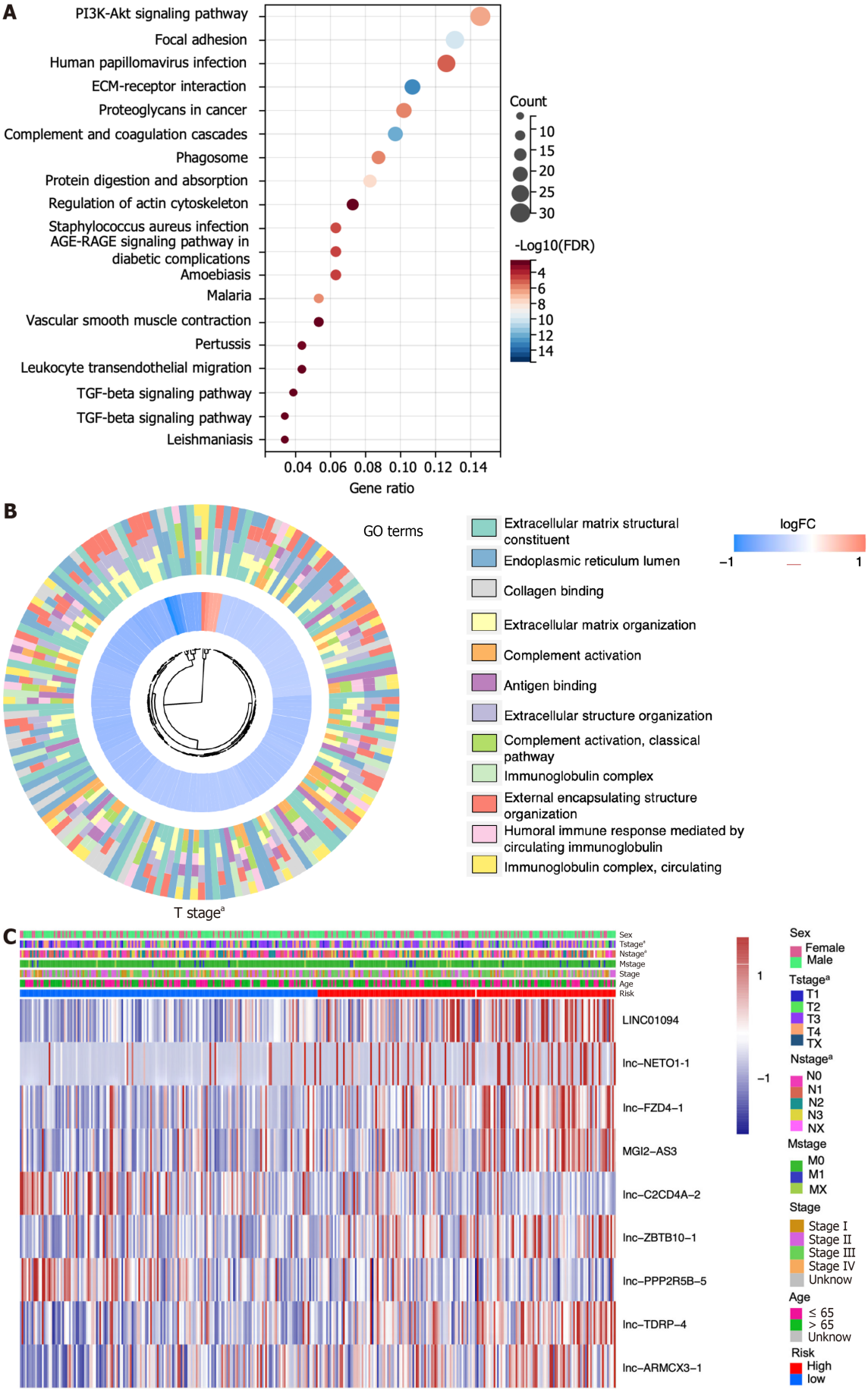

Figure 4 The functional enrichment analysis of differentially expressed genes in high- and low-risk groups was conducted. A and B: The

enrichment of differentially expressed genes between high-risk group and low-risk group was examined using KEGG and GO; C: The heatmap illustrates the relationship between risk score and clinical features ($^{a}P < 0.05$).

clinical characteristics (Figure 2D). This suggested that the risk score might more correctly predict GC patient survival. The AUC was 0.678, 0.692, and 0.702 for predicting the 1-, 2-, and 3-year survival rates, respectively (Figure 2E). DCA evaluation of the clinical value of risk signature revealed that the risk score outperformed clinical factors (Figure 2F).

Of these nine PRLs, only LINC01094 and MAGI2-AS3 were previously reported[42,43]. In glioblastoma and renal clear cell carcinoma, LINC01094 has been widely explored. Poor prognosis is linked to high expression of LINC01094 in renal clear cell carcinoma and glioblastoma. Inhibiting LINC01094 causes these two cancer cells to proliferate, migrate, and invade less often while also increasing apoptosis[44,45]. It has been shown that LINC01094 is a predictor in assessing a patient's prognosis of colon cancer[46]. Its expression level is greater than that of surrounding tissues in colon cancer tumor tissues, and it is connected to vascular invasion, positive lymph node metastases, and TNM stage. The proliferation, invasion, and migration of colon cancer cells can be inhibited by LINC01094 knockdown[47]. Within our research, LINC01094 expression was greater in the HRG, with more advanced T and N stages, compared to the LRG (Figure 4C). Corresponding to the results of autophagy-related lncRNAs in GC, the HR of LINC01094 in our investigation was 1.798, indicating that LINC01094 is an effector that increases the risk of GC[48]. Recent research has shown that LINC01094 is associated with the EMT pathway, macrophage infiltration, and weak prognosis in GC. These findings are in agreement with the findings of our gene enrichment study[49].

MAGI2 antisense RNA 3 (MAGI2-AS3) is abundant in human malignancies, interacts with up to 32 RNAs, and its expression levels correlate with cancer progression and prognosis[50]. However, most existing research focuses on breast, bladder, and lung cancer, and there are only a handful of studies on GC. MAGI2-AS3 expression is reduced in prostate cancer, and MAGI2-AS3 overexpression decreases cell biological processes such as proliferation, migration, and invasion. MAGI2-AS3 also reduces prostate cancer growth *via* regulating miR-142-3p, according to the researchers[51]. MAGI2-AS3 expression is reduced in non-small cell lung cancer tissues. MAGI2-AS3 overexpression decreases NSCLC cell proliferation and invasion, while MAGI2-AS3 inhibition has the reverse effect[52]. Li *et al*[52] found that MAGI2-AS3 is a significant predictor factor for OS and disease-free survival of GC and influences cell migration and invasion processes by favorably influencing the expression of ZEB1[52,53]. In a different research, patients with GC who had low MAGI2-AS3 expression survived noticeably longer than those who had high expression[54]. In our research, In the HRG, MAGI2-AS3 expression was considerably elevated. There are few studies on MAGI2-AS3 in GC, and it is yet unknown how it specifically contributes to the formation and progression of the disease. Following a thorough search, there is no information about lnc-NETO1-1, lnc-FZD4-1, lnc-ZBTB10-1, lnc-TDRP-4, lnc-ARMCX3-1, lnc-C2CD4A-2, lnc-PPP2R5B- 5, and more research will be conducted in the future.

We found that the risk signature was an independent prognostic factor using univariate and multivariate Cox analysis of risk scores and other clinical features (Figure 3A and B). We created a nomogram using tumor stage and risk score to predict patients' 1-, 3-, and 5-year OS (Figure 3C). In former times, many scholars constructed their unique nomogram. Gou *et al*[54] analyzed the operation history, treatment line, lung immune prognostic index, and platelet-to-lymphocyte ratio of immunotherapy-receiving patients with GC metastases to develop a nomogram for assessing the prognosis of these patients[54,55]. Yang *et al*[56] reported a nomogram based on pathological differentiation degree, Lauren type, infiltration depth, lymph node metastasis, tumor deposit, and family history of malignant tumor to predict the prognosis of GC patients[56]. We hope that the nomogram of this study, along with that existing nomogram, will shed fresh light on the prognostic prediction of GC.

The differentially expressed mRNAs in HRG and LRG were primarily enriched in the PI3K-Akt signaling pathway, invasion, and metastasis-related pathways, extracellular matrix-related pathways, and immune response-related pathways, according to KEGG and GO functional enrichment analyses (Figure 4A and B). One of the most essential signaling routes in the cell is the PI3K-Akt signaling system. It is a crucial cancer regulator, and PI3K inhibitors significantly suppress tumor development[57]. The PI3K-Akt pathway is critical in HER2-positive GC[58]. Therefore, we speculate that patients in the HRG may benefit from targeted therapy, which is worthy of further exploration. These results suggest significant molecular functional differences between HRG and LRG in GC. They may provide information for inferring the veiled mechanism of PRLs affecting the prognosis of GC. As a result, we predict that patients in the HRG may profit from targeted treatment, which merits additional investigation. These findings point to substantial molecular functional variations in GC between HRG and LRG. They may give information for deducing the veiled mechanism of PRLs influencing GC prognosis. Therefore, we hypothesize that targeted treatment may be advantageous for patients in the HRG, which merits further investigation. These findings imply important molecular functional variations between differential GC risk groups. They may provide details to deduce how PRLs impact the prognosis of GC in a covert manner.

The immune response is an essential effect of GC occurrence and treatment. The variations in immune cell infiltration between HRG and LRG were calculated using six methods. The findings revealed that the HRG had much larger levels of immune cell infiltration than the LRG (Figure 5A). Further examination of the variations in immune function between HRG and LRG revealed eight statistically significant differences, with the HRG having better immune function (Figure 5B). For instance, the APC co-stimulation function is greater in the HRG; it is the first signal of initial T-cell activation. Under the co-stimulation of two major signals, T cells can fully activate and acquire the capability to proliferate, survive, and produce related cytokines[59]. Tumor antigen presentation by human leukocyte antigen class I (HLA-I) molecules is required for effective CD8+ T cell-dependent tumor cell killing. Higher HLA scores were discovered in the HRG (Figure 5B). Chowell *et al*[60] studied 1535 cancer patients who had received immunotherapy and discovered

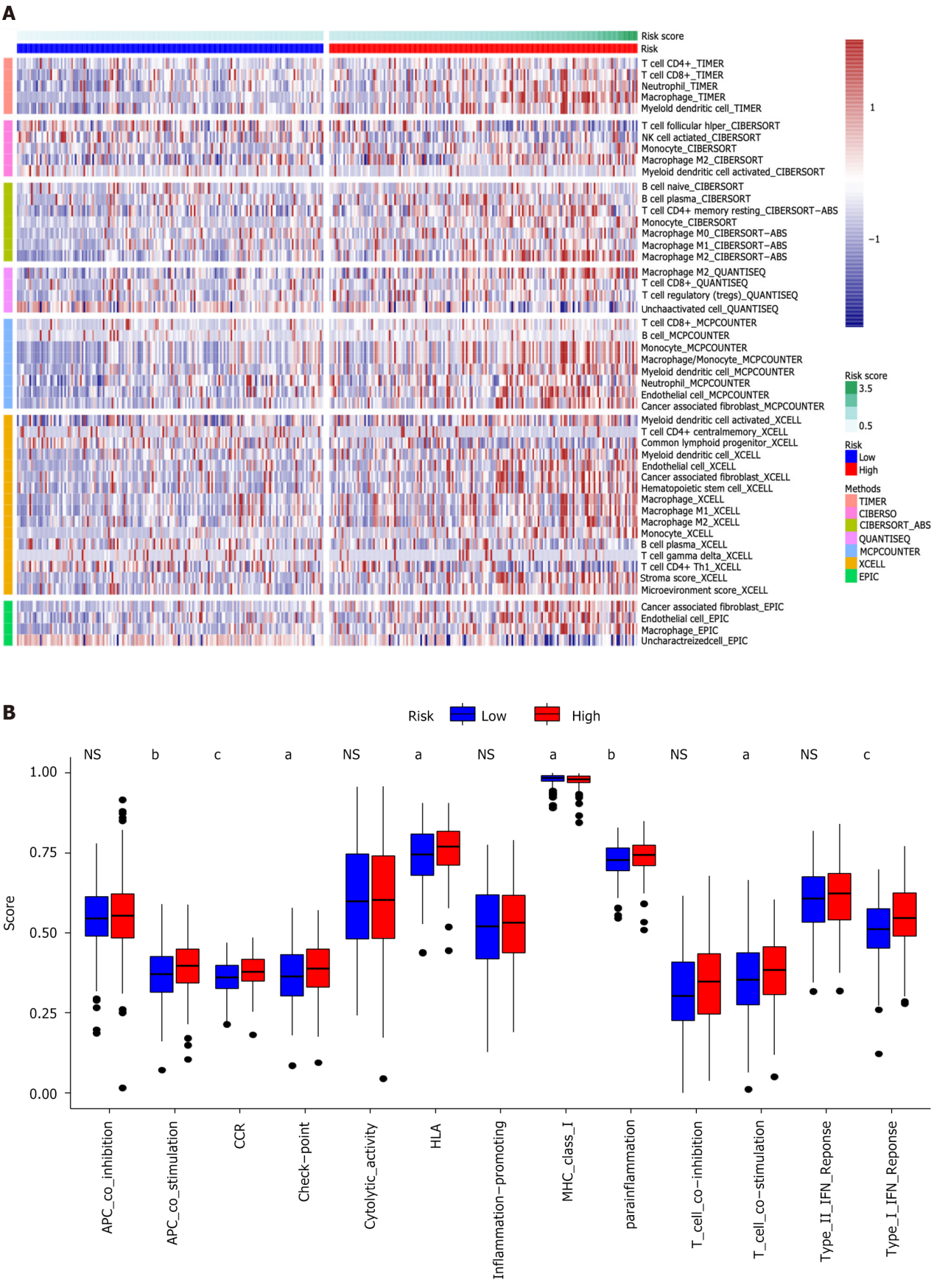
A
Risk score
Risk
T cell CD4+_TIMER
T cell CD8+_TIMER
Neutrophil_TIMER
Macrophage_TIMER
Myeloid dendritic cell_TIMER
T cell follicular hlper_CIBERSORT
NK cell actiated_CIBERSORT
Monocyte_CIBERSORT
Macrophage M2_CIBERSORT
Myeloid dendritic cell activated_CIBERSORT
B cell naive_CIBERSORT
B cell plasma_CIBERSORT
T cell CD4+ memory resting_CIBERSORT−ABS
Monocyte_CIBERSORT
Macrophage M0_CIBERSORT−ABS
Macrophage M1_CIBERSORT−ABS
Macrophage M2_CIBERSORT−ABS
Macrophage M2_QUANTISEQ
T cell CD8+_QUANTISEQ
T cell regulatory (tregs)_QUANTISEQ
Unchaactivated cell_QUANTISEQ
T cell CD8+_MCPCOUNTER
B cell_MCPCOUNTER
Monocyte_MCPCOUNTER
Macrophage/Monocyte_MCPCOUNTER
Myeloid dendritic cell_MCPCOUNTER
Neutrophil_MCPCOUNTER
Endothelial cell_MCPCOUNTER
Cancer associated fibroblast_MCPCOUNTER
Myeloid dendritic cell activated_XCELL
T cell CD4+ centralmemory_XCELL
Common lymphoid progenitor_XCELL
Myeloid dendritic cell_XCELL
Endothelial cell_XCELL
Cancer associated fibroblast_XCELL
Hematopoietic stem cell_XCELL
Macrophage_XCELL
Macrophage M1_XCELL
Macrophage M2_XCELL
Monocyte_XCELL
B cell plasma_XCELL
T cell gamma delta_XCELL
T cell CD4+ Th1_XCELL
Stroma score_XCELL
Microevironment score_XCELL
Cancer associated fibroblast_EPIC
Endothelial cell_EPIC
Macrophage_EPIC
Uncharactreizedcell_EPIC
1
−1
Risk score
3.5
0.5
Risk
Low
High
Methods
TIMER
CIBERSO
CIBERSORT_ABS
QUANTISEQ
MCPCOUNTER
XCELL
EPIC
B
Risk
Low
High
NS
b
c
a
NS
a
NS
a
b
NS
a
NS
c
Score
1.00
0.75
0.50
0.25
0.00
APC_co_inhibition
APC_co_stimulation
CCR
Check−point
Cytolytic_activity
HLA
Inflammation−promoting
MHC_class_I
parainflammation
T_cell_co−inhibition
T_cell_co−stimulation
Type_II_IFN_Reponse
Type_I_IFN_Reponse

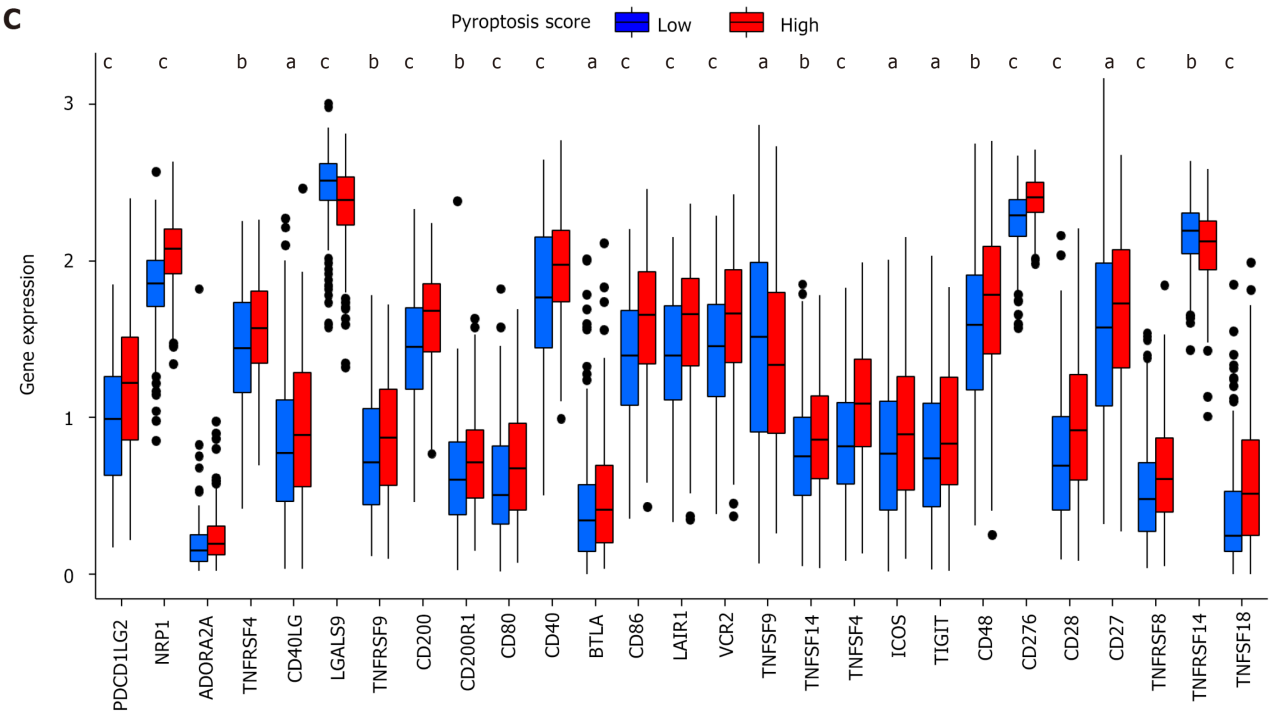

Figure 5 Analyses of immune cell infiltration, immunological function, and immune checkpoints with risk groups. A: Six algorithms to analyze the immune cell infiltration between different risk populations; B and C: Scores for immune function and the expression of immune checkpoints differentiate between those at high-risk group and low-risk group. [a]*P* < 0.05, [b]*P* < 0.01, [c]*P* < 0.001; ns: Not significant; HLA: Human leukocyte antigen.

that the greatest heterozygosity at the HLA-I locus (A, B, C) enhanced OS in patients with advanced cancer following immunotherapy[60]. Concerning checkpoints, the HRG had high levels of most immunological checkpoints, including PDCD1LG2 (PD-L2), TIGIT, BTLA, CD40, and CD80 (Figure 5C). Such findings imply that HRG patients have much more active local immune regulation or immune responses. The risk score may influence the effectiveness of immunotherapy and assist doctors in selecting the individuals who will benefit from it.

Our study has several restrictions. First, the mechanism of PRLs in GC has not been thoroughly investigated in any further molecular biology investigations. Second, no external database was used to verify the signature. The accuracy and dependability of the signature must thus be further validated in a larger sample.

CONCLUSION

Overall, nine PRLs were combined to create a novel signature that may be used to forecast GC patients' prognoses. The signature serves as a clinical predicting tool for immunotherapy in GC patients and may be separated from other clinical variables as an independent prognostic factor.

FOOTNOTES

Author contributions: Wang Y and Li D designed the research; Xun J and Wu Y contributed new reagents/analytic tools; Wang HL analyzed the data; Wang Y wrote the paper; All authors were involved in the critical review of the results and have contributed to read and approved the final manuscript.

Supported by The Scientific Research Project of Integrated Traditional Chinese and Western Medicine of Tianjin Health Commission Administration of Traditional Chinese Medicine, No. 2021010 and No. 2023166; and Xiao-Ping Chen Foundation for the Development of Science and Technology of Hubei Province, No. CXPJJH122002-073.

Conflict-of-interest statement: All the authors report no relevant conflicts of interest for this article.

Country of origin: China

ORCID number: Yu Wang 0000-0001-5031-5121; Hong-Lei Wang 0009-0000-2731-0787.

S-Editor: Li L
L-Editor: A
P-Editor: Zhang XD

REFERENCES

1 **Sung H**, Ferlay J, Siegel RL, Laversanne M, Soerjomataram I, Jemal A, Bray F. Global Cancer Statistics 2020: GLOBOCAN Estimates of Incidence and Mortality Worldwide for 36 Cancers in 185 Countries. *CA Cancer J Clin* 2021; **71**: 209-249 [PMID: 33538338 DOI: 10.3322/caac.21660]
2 **Digklia A**, Wagner AD. Advanced gastric cancer: Current treatment landscape and future perspectives. *World J Gastroenterol* 2016; **22**: 2403-2414 [PMID: 26937129 DOI: 10.3748/wjg.v22.i8.2403]
3 **Wang Z**, Cao L, Zhou S, Lyu J, Gao Y, Yang R. Construction and Validation of a Novel Pyroptosis-Related Four-lncRNA Prognostic Signature Related to Gastric Cancer and Immune Infiltration. *Front Immunol* 2022; **13**: 854785 [PMID: 35392086 DOI: 10.3389/fimmu.2022.854785]
4 **Lv X**, Zhang L, Huang R, Song W. A clinical exploration of neoadjuvant chemotherapy with tegafur, gimeracil, and oteracil potassium capsules combined with oxaliplatin for advanced gastric cancer. *Int J Clin Exp Med* 2015; **8**: 19030-19036 [PMID: 26770529]
5 **Tan Z**. Recent Advances in the Surgical Treatment of Advanced Gastric Cancer: A Review. *Med Sci Monit* 2019; **25**: 3537-3541 [PMID: 31080234 DOI: 10.12659/MSM.916475]
6 **Jim MA**, Pinheiro PS, Carreira H, Espey DK, Wiggins CL, Weir HK. Stomach cancer survival in the United States by race and stage (2001-2009): Findings from the CONCORD-2 study. *Cancer* 2017; **123** Suppl 24: 4994-5013 [PMID: 29205310 DOI: 10.1002/cncr.30881]
7 **Cookson BT**, Brennan MA. Pro-inflammatory programmed cell death. *Trends Microbiol* 2001; **9**: 113-114 [PMID: 11303500 DOI: 10.1016/s0966-842x(00)01936-3]
8 **Huang C**, Li J, Zhang C. What role does pyroptosis play in cancer? *Mol Metab* 2022; **65**: 101587 [PMID: 36055576 DOI: 10.1016/j.molmet.2022.101587]
9 **Ding J**, Wang K, Liu W, She Y, Sun Q, Shi J, Sun H, Wang DC, Shao F. Erratum: Pore-forming activity and structural autoinhibition of the gasdermin family. *Nature* 2016; **540**: 150 [PMID: 27706141 DOI: 10.1038/nature20106]
10 **Yang D**, He Y, Muñoz-Planillo R, Liu Q, Núñez G. Caspase-11 Requires the Pannexin-1 Channel and the Purinergic P2X7 Pore to Mediate Pyroptosis and Endotoxic Shock. *Immunity* 2015; **43**: 923-932 [PMID: 26572062 DOI: 10.1016/j.immuni.2015.10.009]
11 **Yu P**, Zhang X, Liu N, Tang L, Peng C, Chen X. Pyroptosis: mechanisms and diseases. *Signal Transduct Target Ther* 2021; **6**: 128 [PMID: 33776057 DOI: 10.1038/s41392-021-00507-5]
12 **Rogers C**, Erkes DA, Nardone A, Aplin AE, Fernandes-Alnemri T, Alnemri ES. Gasdermin pores permeabilize mitochondria to augment caspase-3 activation during apoptosis and inflammasome activation. *Nat Commun* 2019; **10**: 1689 [PMID: 30976076 DOI: 10.1038/s41467-019-09397-2]
13 **Sannino F**, Sansone C, Galasso C, Kildgaard S, Tedesco P, Fani R, Marino G, de Pascale D, Ianora A, Parrilli E, Larsen TO, Romano G, Tutino ML. Pseudoalteromonas haloplanktis TAC125 produces 4-hydroxybenzoic acid that induces pyroptosis in human A459 Lung adenocarcinoma cells. *Sci Rep* 2018; **8**: 1190 [PMID: 29352134 DOI: 10.1038/s41598-018-19536-2]
14 **Miguchi M**, Hinoi T, Shimomura M, Adachi T, Saito Y, Niitsu H, Kochi M, Sada H, Sotomaru Y, Ikenoue T, Shigeyasu K, Tanakaya K, Kitadai Y, Sentani K, Oue N, Yasui W, Ohdan H. Gasdermin C Is Upregulated by Inactivation of Transforming Growth Factor β Receptor Type II in the Presence of Mutated Apc, Promoting Colorectal Cancer Proliferation. *PLoS One* 2016; **11**: e0166422 [PMID: 27835699 DOI: 10.1371/journal.pone.0166422]
15 **Tu S**, Bhagat G, Cui G, Takaishi S, Kurt-Jones EA, Rickman B, Betz KS, Penz-Oesterreicher M, Bjorkdahl O, Fox JG, Wang TC. Overexpression of interleukin-1beta induces gastric inflammation and cancer and mobilizes myeloid-derived suppressor cells in mice. *Cancer Cell* 2008; **14**: 408-419 [PMID: 18977329 DOI: 10.1016/j.ccr.2008.10.011]
16 **Wang CJ**, Tang L, Shen DW, Wang C, Yuan QY, Gao W, Wang YK, Xu RH, Zhang H. The expression and regulation of DFNA5 in human hepatocellular carcinoma DFNA5 in hepatocellular carcinoma. *Mol Biol Rep* 2013; **40**: 6525-6531 [PMID: 24154762 DOI: 10.1007/s11033-013-2581-8]
17 **Cheng D**, Weckerle A, Yu Y, Ma L, Zhu X, Murea M, Freedman BI, Parks JS, Shelness GS. Biogenesis and cytotoxicity of APOL1 renal risk variant proteins in hepatocytes and hepatoma cells. *J Lipid Res* 2015; **56**: 1583-1593 [PMID: 26089538 DOI: 10.1194/jlr.M059733]
18 **Bostanci V**, Toker H, Senel S, Poyraz O, Akpinar A, Görgün EP, Bakar O. Evaluation of IL-1β, IL-1ra, and IL-10 Levels and outcome of periodontal therapy in chronic periodontitis with familial Mediterranean fever. *Clin Oral Investig* 2017; **21**: 469-475 [PMID: 27068409 DOI: 10.1007/s00784-016-1816-1]
19 **So D**, Shin HW, Kim J, Lee M, Myeong J, Chun YS, Park JW. Cervical cancer is addicted to SIRT1 disarming the AIM2 antiviral defense. *Oncogene* 2018; **37**: 5191-5204 [PMID: 29844574 DOI: 10.1038/s41388-018-0339-4]
20 **Liu Y**, Fang Y, Chen X, Wang Z, Liang X, Zhang T, Liu M, Zhou N, Lv J, Tang K, Xie J, Gao Y, Cheng F, Zhou Y, Zhang Z, Hu Y, Zhang X, Gao Q, Zhang Y, Huang B. Gasdermin E-mediated target cell pyroptosis by CAR T cells triggers cytokine release syndrome. *Sci Immunol* 2020; **5** [PMID: 31953257 DOI: 10.1126/sciimmunol.aax7969]
21 **Luo X**, Zhang X, Gan L, Zhou C, Zhao T, Zeng T, Liu S, Xiao Y, Yu J, Zhao F. The outer membrane protein Tp92 of Treponema pallidum induces human mononuclear cell death and IL-8 secretion. *J Cell Mol Med* 2018; **22**: 6039-6054 [PMID: 30596396 DOI: 10.1111/jcmm.13879]
22 **St Laurent G**, Wahlestedt C, Kapranov P. The Landscape of long noncoding RNA classification. *Trends Genet* 2015; **31**: 239-251 [PMID: 25869999 DOI: 10.1016/j.tig.2015.03.007]
23 **Tragante V**, Moore JH, Asselbergs FW. The ENCODE project and perspectives on pathways. *Genet Epidemiol* 2014; **38**: 275-280 [PMID: 24723339 DOI: 10.1002/gepi.21802]
24 **Batista PJ**, Chang HY. Long noncoding RNAs: cellular address codes in development and disease. *Cell* 2013; **152**: 1298-1307 [PMID: 23498938 DOI: 10.1016/j.cell.2013.02.012]

25 **Han X**, Zhang S. Role of Long Non-Coding RNA LINC00641 in Cancer. *Front Oncol* 2021; **11**: 829137 [PMID: 35155216 DOI: 10.3389/fonc.2021.829137]

26 **Yan H**, Bu P. Non-coding RNA in cancer. *Essays Biochem* 2021; **65**: 625-639 [PMID: 33860799 DOI: 10.1042/EBC20200032]

27 **Hombach S**, Kretz M. Non-coding RNAs: Classification, Biology and Functioning. *Adv Exp Med Biol* 2016; **937**: 3-17 [PMID: 27573892 DOI: 10.1007/978-3-319-42059-2_1]

28 **Yang L**, Lin C, Jin C, Yang JC, Tanasa B, Li W, Merkurjev D, Ohgi KA, Meng D, Zhang J, Evans CP, Rosenfeld MG. lncRNA-dependent mechanisms of androgen-receptor-regulated gene activation programs. *Nature* 2013; **500**: 598-602 [PMID: 23945587 DOI: 10.1038/nature12451]

29 **Hung CL**, Wang LY, Yu YL, Chen HW, Srivastava S, Petrovics G, Kung HJ. A long noncoding RNA connects c-Myc to tumor metabolism. *Proc Natl Acad Sci U S A* 2014; **111**: 18697-18702 [PMID: 25512540 DOI: 10.1073/pnas.1415669112]

30 **Kim J**, Piao HL, Kim BJ, Yao F, Han Z, Wang Y, Xiao Z, Siverly AN, Lawhon SE, Ton BN, Lee H, Zhou Z, Gan B, Nakagawa S, Ellis MJ, Liang H, Hung MC, You MJ, Sun Y, Ma L. Long noncoding RNA MALAT1 suppresses breast cancer metastasis. *Nat Genet* 2018; **50**: 1705-1715 [PMID: 30349115 DOI: 10.1038/s41588-018-0252-3]

31 **Endo H**, Shiroki T, Nakagawa T, Yokoyama M, Tamai K, Yamanami H, Fujiya T, Sato I, Yamaguchi K, Tanaka N, Iijima K, Shimosegawa T, Sugamura K, Satoh K. Enhanced expression of long non-coding RNA HOTAIR is associated with the development of gastric cancer. *PLoS One* 2013; **8**: e77070 [PMID: 24130837 DOI: 10.1371/journal.pone.0077070]

32 **Wang Y**, Chen X, Jiang F, Shen Y, Fang F, Li Q, Yang C, Dong Y, Shen X. A prognostic signature of pyroptosis-related lncRNAs verified in gastric cancer samples to predict the immunotherapy and chemotherapy drug sensitivity. *Front Genet* 2022; **13**: 939439 [PMID: 36147488 DOI: 10.3389/fgene.2022.939439]

33 **Li T**, Fan J, Wang B, Traugh N, Chen Q, Liu JS, Li B, Liu XS. TIMER: A Web Server for Comprehensive Analysis of Tumor-Infiltrating Immune Cells. *Cancer Res* 2017; **77**: e108-e110 [PMID: 29092952 DOI: 10.1158/0008-5472.CAN-17-0307]

34 **Chen B**, Khodadoust MS, Liu CL, Newman AM, Alizadeh AA. Profiling Tumor Infiltrating Immune Cells with CIBERSORT. *Methods Mol Biol* 2018; **1711**: 243-259 [PMID: 29344893 DOI: 10.1007/978-1-4939-7493-1_12]

35 **Plattner C**, Finotello F, Rieder D. Deconvoluting tumor-infiltrating immune cells from RNA-seq data using quanTIseq. *Methods Enzymol* 2020; **636**: 261-285 [PMID: 32178821 DOI: 10.1016/bs.mie.2019.05.056]

36 **Becht E**, Giraldo NA, Lacroix L, Buttard B, Elarouci N, Petitprez F, Selves J, Laurent-Puig P, Sautès-Fridman C, Fridman WH, de Reyniès A. Estimating the population abundance of tissue-infiltrating immune and stromal cell populations using gene expression. *Genome Biol* 2016; **17**: 218 [PMID: 27765066 DOI: 10.1186/s13059-016-1070-5]

37 **Aran D**, Hu Z, Butte AJ. xCell: digitally portraying the tissue cellular heterogeneity landscape. *Genome Biol* 2017; **18**: 220 [PMID: 29141660 DOI: 10.1186/s13059-017-1349-1]

38 **Racle J**, Gfeller D. EPIC: A Tool to Estimate the Proportions of Different Cell Types from Bulk Gene Expression Data. *Methods Mol Biol* 2020; **2120**: 233-248 [PMID: 32124324 DOI: 10.1007/978-1-0716-0327-7_17]

39 **Chia NY**, Tan P. Molecular classification of gastric cancer. *Ann Oncol* 2016; **27**: 763-769 [PMID: 26861606 DOI: 10.1093/annonc/mdw040]

40 **Li K**, Zhang A, Li X, Zhang H, Zhao L. Advances in clinical immunotherapy for gastric cancer. *Biochim Biophys Acta Rev Cancer* 2021; **1876**: 188615 [PMID: 34403771 DOI: 10.1016/j.bbcan.2021.188615]

41 **Dong X**, Fu X, Yu M, Li Z. Long Intergenic Non-Protein Coding RNA 1094 Promotes Initiation and Progression of Glioblastoma by Promoting microRNA-577-Regulated Stabilization of Brain-Derived Neurotrophic Factor. *Cancer Manag Res* 2020; **12**: 5619-5631 [PMID: 32765065 DOI: 10.2147/CMAR.S256147]

42 **Jiang Y**, Zhang H, Li W, Yan Y, Yao X, Gu W. FOXM1-Activated LINC01094 Promotes Clear Cell Renal Cell Carcinoma Development *via* MicroRNA 224-5p/CHSY1. *Mol Cell Biol* 2020; **40** [PMID: 31767633 DOI: 10.1128/MCB.00357-19]

43 **Zhu B**, Liu W, Liu H, Xu Q, Xu W. LINC01094 Down-Regulates miR-330-3p and Enhances the Expression of MSI1 to Promote the Progression of Glioma. *Cancer Manag Res* 2020; **12**: 6511-6521 [PMID: 32801889 DOI: 10.2147/CMAR.S254630]

44 **Li XX**, Yu Q. Linc01094 Accelerates the Growth and Metastatic-Related Traits of Glioblastoma by Sponging miR-126-5p. *Onco Targets Ther* 2020; **13**: 9917-9928 [PMID: 33116576 DOI: 10.2147/OTT.S263091]

45 **Xu H**, Wang X, Wu J, Ji H, Chen Z, Guo H, Hou J. Long Non-coding RNA LINC01094 Promotes the Development of Clear Cell Renal Cell Carcinoma by Upregulating SLC2A3 *via* MicroRNA-184. *Front Genet* 2020; **11**: 562967 [PMID: 33173535 DOI: 10.3389/fgene.2020.562967]

46 **Zhang G**, Gao Y, Yu Z, Su H. Upregulated long intergenic non-protein coding RNA 1094 (LINC01094) is linked to poor prognosis and alteration of cell function in colorectal cancer. *Bioengineered* 2022; **13**: 8526-8537 [PMID: 35287563 DOI: 10.1080/21655979.2022.2051839]

47 **Wang W**, Pei Q, Wang L, Mu T, Feng H. Construction of a Prognostic Signature of 10 Autophagy-Related lncRNAs in Gastric Cancer. *Int J Gen Med* 2022; **15**: 3699-3710 [PMID: 35411177 DOI: 10.2147/IJGM.S348943]

48 **Ye Y**, Ge O, Zang C, Yu L, Eucker J, Chen Y. LINC01094 Predicts Poor Prognosis in Patients With Gastric Cancer and is Correlated With EMT and Macrophage Infiltration. *Technol Cancer Res Treat* 2022; **21**: 15330338221080977 [PMID: 35254147 DOI: 10.1177/15330338221080977]

49 **Kai-Xin L**, Cheng C, Rui L, Zheng-Wei S, Wen-Wen T, Peng X. Roles of lncRNA MAGI2-AS3 in human cancers. *Biomed Pharmacother* 2021; **141**: 111812 [PMID: 34126355 DOI: 10.1016/j.biopha.2021.111812]

50 **Hu R**, Wu P, Liu J. LncRNA MAGI2-AS3 Inhibits Prostate Cancer Progression by Targeting the miR-142-3p. *Horm Metab Res* 2022; **54**: 754-759 [PMID: 35944561 DOI: 10.1055/a-1891-6864]

51 **Gong J**, Ma L, Peng C, Liu J. LncRNA MAGI2-AS3 acts as a tumor suppressor that attenuates non-small cell lung cancer progression by targeting the miR-629-5p/TXNIP axis. *Ann Transl Med* 2021; **9**: 1793 [PMID: 35071487 DOI: 10.21037/atm-21-6466]

52 **Li D**, Wang J, Zhang M, Hu X, She J, Qiu X, Zhang X, Xu L, Liu Y, Qin S. LncRNA MAGI2-AS3 Is Regulated by BRD4 and Promotes Gastric Cancer Progression *via* Maintaining ZEB1 Overexpression by Sponging miR-141/200a. *Mol Ther Nucleic Acids* 2020; **19**: 109-123 [PMID: 31837602 DOI: 10.1016/j.omtn.2019.11.003]

53 **Zhang X**, Jiang Y, Xie Y, Leng X, Song F. Comprehensive Analysis of lncRNAs Associated with the Pathogenesis and Prognosis of Gastric Cancer. *DNA Cell Biol* 2020; **39**: 299-309 [PMID: 31934786 DOI: 10.1089/dna.2019.5161]

54 **Gou M**, Qian N, Zhang Y, Wei L, Fan Q, Wang Z, Dai G. Construction of a nomogram to predict the survival of metastatic gastric cancer patients that received immunotherapy. *Front Immunol* 2022; **13**: 950868 [PMID: 36225924 DOI: 10.3389/fimmu.2022.950868]

55 **Wang F**, Fan L, Zhao Q, Liu Y, Zhang Z, Wang D, Zhao X, Li Y, Tan B. Family history of malignant tumor is a predictor of gastric cancer prognosis: Incorporation into a nomogram. *Medicine (Baltimore)* 2022; **101**: e30141 [PMID: 36107576 DOI:

10.1097/MD.0000000000030141]

56 **Yang J**, Nie J, Ma X, Wei Y, Peng Y, Wei X. Targeting PI3K in cancer: mechanisms and advances in clinical trials. *Mol Cancer* 2019; **18**: 26 [PMID: 30782187 DOI: 10.1186/s12943-019-0954-x]

57 **Sukawa Y**, Yamamoto H, Nosho K, Ito M, Igarashi H, Naito T, Mitsuhashi K, Matsunaga Y, Takahashi T, Mikami M, Adachi Y, Suzuki H, Shinomura Y. HER2 expression and PI3K-Akt pathway alterations in gastric cancer. *Digestion* 2014; **89**: 12-17 [PMID: 24458107 DOI: 10.1159/000356201]

58 **Dustin ML**. The immunological synapse. *Cancer Immunol Res* 2014; **2**: 1023-1033 [PMID: 25367977 DOI: 10.1158/2326-6066.CIR-14-0161]

59 **Chowell D**, Morris LGT, Grigg CM, Weber JK, Samstein RM, Makarov V, Kuo F, Kendall SM, Requena D, Riaz N, Greenbaum B, Carroll J, Garon E, Hyman DM, Zehir A, Solit D, Berger M, Zhou R, Rizvi NA, Chan TA. Patient HLA class I genotype influences cancer response to checkpoint blockade immunotherapy. *Science* 2018; **359**: 582-587 [PMID: 29217585 DOI: 10.1126/science.aao4572]

60 **Chowell D**, Krishna C, Pierini F, Makarov V, Rizvi NA, Kuo F, Morris LGT, Riaz N, Lenz TL, Chan TA. Evolutionary divergence of HLA class I genotype impacts efficacy of cancer immunotherapy. *Nat Med* 2019; **25**: 1715-1720 [PMID: 31700181 DOI: 10.1038/s41591-019-0639-4]

Published by **Baishideng Publishing Group Inc**
7041 Koll Center Parkway, Suite 160, Pleasanton, CA 94566, USA
Telephone: +1-925-3991568
E-mail: office@baishideng.com
Help Desk: https://www.f6publishing.com/helpdesk
https://www.wjgnet.com